Grain-Oriented Steel Rings for an Experimental Comparison of Relative Magnetostriction and Maxwell's Forces Effects

Remi Penin, Jean-Philippe Lecointe, Guillaume Parent, Jean-Francois Brudny, Thierry Belgrand

HAL Id: hal-03350810
https://univ-artois.hal.science/hal-03350810

Submitted on 18 May 2022

Grain Oriented Steel Rings for an Experimental Comparison of Relative Magnetostriction and Maxwell's Forces Effects

R. Penin, J-Ph. Lecointe, G. Parent, J-F.Brudny, T. Belgrand

Abstract—**The magnetic material quality of transformer cores influences their emitted acoustic noise. The latter is generated by vibrations resulting from the effects of the Maxwell's forces, located in the corners, and the magnetostriction inside the magnetic steel. In this paper, two annular structures allow differentiating these two phenomena and analyzing the vibration origins. Then, two different materials are compared, leading to conclusions about the influence of the material anisotropy on vibrations. At last, the measured vibration components are fully justified with the local saturation effects.**

Index Terms—**Displacement measurement, Magnetic anisotropy, magnetic flux density, magnetic forces, magnetostriction, soft magnetic materials, transformer cores, vibrations.**

NOMENCLATURE

a : Acceleration
l : Material length
n_2 : Secondary winding turn number
p : Pressure of Maxwell's forces
B : Magnetic flux density in the core
B_e : Air gap magnetic flux density
GO : Grain Oriented
RD : Rolling Direction
S : Stack cross section
TD : Transverse Direction
β : Shifting angle
γ : Angle between the measurement direction and for RD of the first sheet of a stack

V_2 : Sinusoidal secondary RMS voltage
α : Anisotropic angle of applied field
μ_0 : Vacuum permeability ($4\pi 10^{-7}$H/m)
θ : Angle between the measurement and the RD
ω : Angular frequency (frequency f)

I. INTRODUCTION

The acoustic noise emitted by transformers results from many contributions. Indeed, the magnetic core composed of electrical steel sheets is source of high concern for the steel producers and the transformer manufacturers [1]-[2]. The noise emission results from vibrations, which have two different origins: the Maxwell's forces due to effects between laminations [3] and the magnetostriction due to the specific behaviour of the electrical steel [4]-[5]. Thus, it is a challenge to separate the influence of these two factors and to weight their respective contribution to the emitted noise when Grain Oriented (GO) steel is used to build the magnetic circuit [6]-[7].

The first part of the paper presents the phenomenon of magnetostriction and the forces arising between the sheets. Then, the second part describes the test bench composed of stacked GO electrical steel rings [8]-[9]. The results are presented and discussed in the third part. The main contribution concerns the effect distinction of the Maxwell's forces and the magnetostriction. Hints are given for understanding the noise generation in transformers. Two qualities of electrical steel, i.e. a conventional GO electrical steel (denoted CGO) and a high permeability GO one (denoted HGO), are also compared to quantify the influences of the anisotropy on the vibrations. In order to explain every vibration components, the authors analyse the impact of the supply voltage harmonics [10]-[11] and the effects of local saturations in the magnetic circuit [12].

II. MAGNETOSTRICTION AND MAXWELL'S FORCES

The Maxwell's forces are generated by the presence of magnetic flux across the air gap between the magnetic steel laminations. It is particularly the case in the transformer corners because in this area, the magnetic field has to change direction and, due to the high anisotropy of GO electrical steel, it has to cross the air gaps existing between the latter, creating magnetic discontinuities. Indeed, the field can remain

in the same plane or pass from one layer to another depending on permeability situation [13]. Moreover, two potential sources for Maxwell forces exist: in plane (Fig. 1(b) way 1) due to the distributed air gap of the step lap arrangement (Fig. 1(a)) and out of the plane (Fig. 1(b) way 2) due to the air gap brought by the insulation layer intrinsic to the steel [14]-[15]. This paper is focused on the second case.

The p pressure corresponding to the Maxwell's forces interacting between two successive laminations can be expressed as follows:

$$p = \frac{B_e^2}{2\mu_0} \qquad (1)$$

Expression (1) shows that p components contain a prevailing term of fundamental frequency twice the value of the excitation one. This study will be focused on vibrations induced by all p components, the corresponding induced external displacements being tied to the mechanical response of the structure.
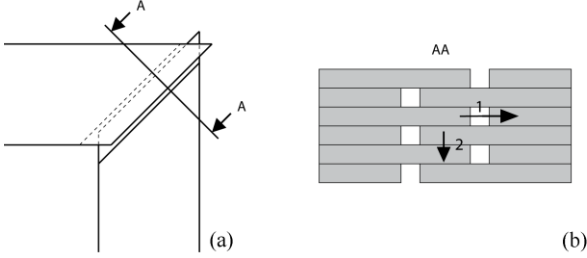

Fig. 1.   Joint region in conventional single step lap assembling

The magnetostriction appears due to the magnetization of the electrical steel sheets. It takes place when the domains have to rotate to align themselves along the direction of the magnetic field. This is particularly the case in the transformer joints where the magnetic field concentrates at the inner part of the corners and makes its magnitude high enough to locally move the domains [16].

Magnetostriction is generally expressed as a relative deformation $\frac{\Delta l}{l}$ which depends, for a single crystal, on the magnetostriction coefficients λ_{100} and λ_{111}, respectively 23.7×10^{-6} and -4.1×10^{-6} for the case of the GO structure [17].

Let us denote α the anisotropic angle of applied field with respect to the Rolling Direction (RD), which will be marked with a bold arrow in the figures, and θ the angle between the measurement direction and the RD. For θ from 0° to 55°, the magnetostriction is negative, and so the sheet is contracting. On the other hand, for θ from 55° to 90°, the magnetostriction is positive and so the sheet is stretching. The deformation amplitude varies with α [18]: it is very low when $\alpha = 0°$ and it increases with α. These behaviours are due to a low field magnetostriction. This specificity can be easily visualized thanks to the so-called "butterfly loop" graphs [19]. Fig. 2 shows the link between the magnitude of the relative deformations of a sheet due to the magnetostriction depending on α and θ. The displacements in the RD have amplitudes

higher than those in the Transverse Direction (TD) and no deformation around 55°. Since magnetostriction is at constant volume, the deformations in the outer plane direction are consequences of the in-plane ones. That means that the lamination presents a deformation according to its thickness [20]. Like Maxwell's forces, prevailing vibrations due to magnetostriction present a fundamental frequency twice the excitation [21].
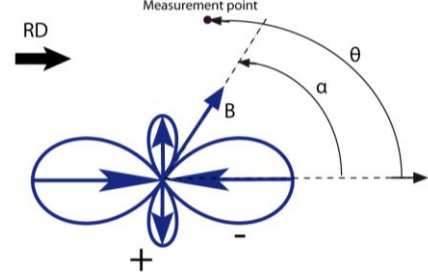

Fig. 2.   GO steel sheet variations with α and θ of the relative elongation/compression due to magnetostriction.

III.   TEST BENCH

A.   Ring Structure

The experimental device presented in this paper deals with stacks of rings built with GO electrical steel subjected to a circumferential magnetisation. Each ring of the stack is shifted from the previous one by a constant β angle (Fig. 3). This structure is able to give an image of the magnetic behavior of a transformer corner joint when the Maxwell's forces in plane are assumed to be null.

Axial (along z) and radial (along y) vibrations are analysed in this study considering $\beta = 0°$ and $\beta = 90°$.

Case of axial vibrations:
- For $\beta = 0°$, there is no reason for the field to move from one layer to another since all rings are stacked with their RD parallel. In that way no Maxwell's force takes place between the sheets and the only possible deformations is related to magnetostriction.
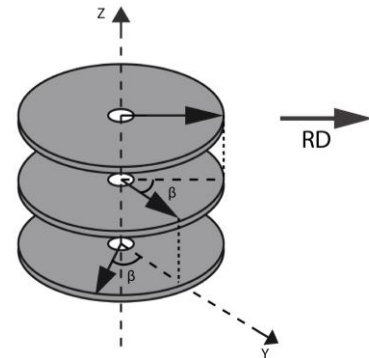

Fig. 3.   Stack of shifted rings

- For $\beta = 90°$ between successive layers, the magnetic flux is established according to the RD of lamination and passes through the interlaminar air gap to reach the RD of the adjoining laminations [22]. Hence, deformations will result from a mix of Maxwell's forces and magnetostriction.

Moreover, Maxwell's force amplitudes will be maximum.

Case of Radial Vibrations:

The radial vibrations are caused, whatever the shifting, only by the magnetostrictive effect.

B. Test Bench Presentation

The experimental device has been designed to maximize the reliability of the measurements (Fig. 4.). The two stack configurations are mounted inside the same frame structure. The stacks can be rotated around the stacking direction axis.
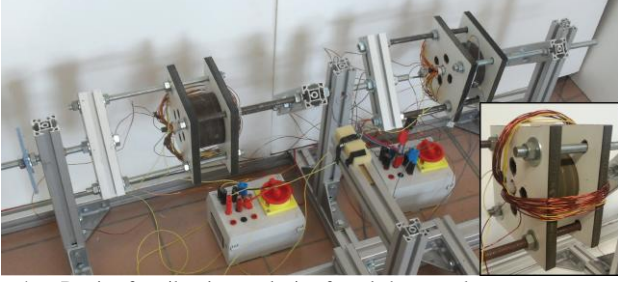

Fig. 4.   Device for vibration analysis of steel sheet stacks

Two steel qualities have been tested (Fig. 5): the first one is GO "PowerCore C" electrical steel of 0,35mm nominal thickness (174 sheets for each stack) called "CGO" and the second one is GO "PowerCore H" electrical steel of 0,30mm nominal thickness (203 sheets for each stack) called "HGO" [23]. The HGO permeability in the RD is higher and it is more anisotropic [24]. The sheets are of internal radius 8mm and of outside radius 50mm. The sheet insulation is around 5μm. The sheets are clamped between two non magnetic bakelite A and B plates and maintained with threaded rods. The tightening torque applied on the nuts is controlled with a torque wrench and is the same for each stack and for every test.
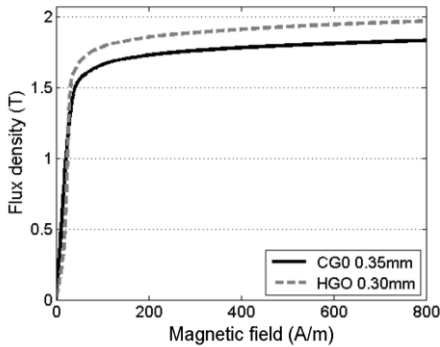

Fig. 5.   Magnetic characteristics in the RD of the used materials

Holes have been drilled through the bakelite plates for sensors access in order to record the axial deformations of the stacks (Fig. 4). The measurements points A_1 to A_4 and B_1 to B_4 are presented in Fig. 6(a) (holes face to face are numbered in the same way).

The spatial reference for the radial measurements is the RD of the first sheet of a stack (against the plate A), which is aligned along the x'x axis of the holes noted 1 and 3 (Fig. 6(b)).

The radial measured point is located with the γ angle with respect to this reference.

For the shifted structure, $\gamma = 0°$ correspond to RD for every two sheets. The excitation is provided by a primary 28 turn winding creating a circumferential magnetisation. A 10 turn secondary winding allows measuring the average flux density in the core. Those windings are distributed on one half of the structure only (Fig. 4) in order to apply the measuring devices. The primary winding is supplied with a 50Hz sinusoidal voltage provided by an auto-transformer (Total Harmonic Distortion < 3%). Hence, the devices are submitted to a unidirectional field.
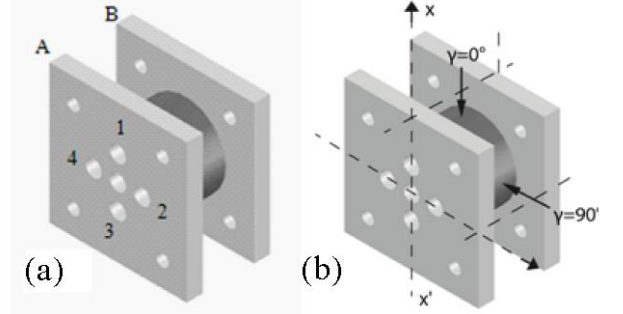

Fig. 6.   Axial and Radial measuring points

Finally, the magnetic flux density in the core is computed from the secondary voltage through the following formula:

$$B = \frac{V_2 \sqrt{2}}{n_2 \omega S} \qquad (2)$$

The measurements have been done for magnetic flux density values of 0.7T, 1.1T and 1.5T. A Bruël and Kjaer PULSE data acquisition system is used in order to analyze signals measured with mono-axial accelerometers.

IV. Experimental results

A. Measurements of Axial Vibrations

The accelerations of the deformations are presented for the CGO in Fig. 7 for the 100 Hz frequency component only for points A_1 to A_4 of the non-shifted structure with the magnetic flux density value of 1.1T. Theoretically, for both configurations, according to symmetries, points A_1 and A_3 should present the same vibrations. The same remark can also be done for points A_2 and A_4. But, differences between these points are measured; this comes from the uncertainty of the accelerometer placement. To reduce this, an averaging measured values on points 1 and 3 as well as on points 2 and 4 is made for plates A and B. Fig. 8 shows this averaging for both configurations ($\beta = 0°$ and $\beta = 90°$) and both qualities of steel denoting, for example, A_1-A_3 the averaging of measurements made on A_1 and A_3.

It appears that the non-shifted structure ($\beta = 0°$) presents higher vibration levels that the shifted one. It can be explained as follow:

- The Maxwell's forces arising in the case of the shifted configuration induce a contraction of the interlaminar air gaps which limits the mechanical displacements [25].
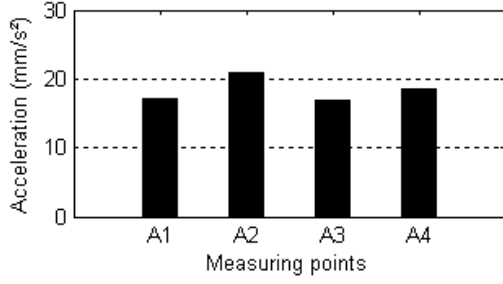- The flux density distribution is different in the shifted stacks

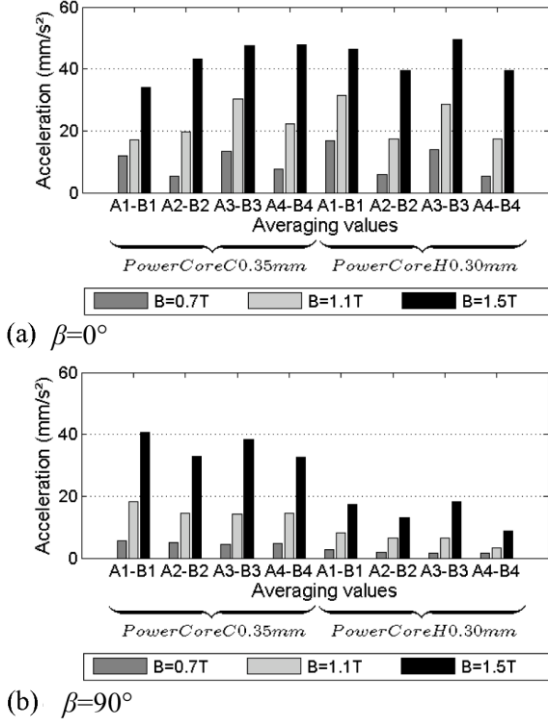Fig 7: Measurements of axial vibrations for plate A ($B = 1.1T$)

(a) β=0°

(b) β=90°

Fig. 8.   Measurements of axial vibrations for non-shifted and shifted stacks

(a) β=0°

(b) β=90°

Fig. 9.   Measurements of radial vibrations for non-shifted and shifted stacks

because the magnetic flux follows the less reluctant path. The authors show in [22] that the flux crosses the air gaps to flow mainly in the RD. Hence α is low, that lead to lower magnetostriction effects.
- Both phenomena (magnetostriction and Maxwell's forces) can compensate each other at a given frequency, explaining the observed vibration differences.

Concerning the difference between the two qualities, the axial and radial vibrations are lower for the HGO shifted stack than for the CGO shifted stack. It can be explained by the fact that the effects of the magnetostriction and the Maxwell's force effects are better compensated and by the fact that the HGO magnetostriction characteristics lead to lower deformations.

It is interesting to note that, for HGO and CGO, the non-shifted structure for 0.7T have the more important vibrations in positions A_1-A_3 and B_1-B_3. Indeed, these points correspond to zones where the flux is in the TD of the sheets. Hence, the magnetostrictive effect is the highest. For $\beta = 90°$, these vibrations are the same for all positions.
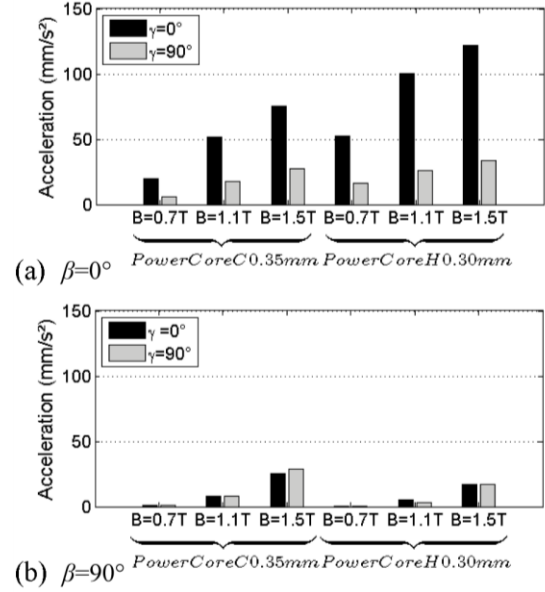
B. Radial Vibration Measurements

For those measurements, the accelerometers are placed on the edges of the stacks for $\gamma = 0°$ and $\gamma = 90°$ (Fig. 6(b)). The results are presented in Fig. 9 for the 100Hz frequency component and for $\beta = 0°$ and $\beta = 90°$.

Whatever the value of the β angle is, the radial vibrations are always due to magnetostriction. For the non-shifted setup, the vibrations occurring along the RD are bigger than the ones across the TD. This is in accordance with the "butter-fly" loops previously mentioned. Moreover, vibrations in the shifted setup are fairly identical for both $\gamma = 0°$ and $\gamma = 90°$.

Concerning the difference between the two qualities, the HGO leads to higher vibrations than the CGO for the non-shifted structure. That can be explained by the strong anisotropy of the material, which generates vibrations of high amplitudes when the magnetic flux is established in the TD. On the contrary, the HGO shifted structure presents lower vibrations than the CGO. The Fig. 9 highlights noteworthy acceleration amplitude differences with the shifting. Indeed, the CGO shifted setup for 0.7T shows that amplitudes are divided by 27 and 8.3 respectively for $\gamma = 0°$ and $\gamma = 90°$. Nevertheless, the ratios decrease when the magnetic flux density value increases: 6.6 and 2.2 for 1.1T and 3 and 0.95 for 1.5T. For the HGO quality, theses ratios are respectively 81 and 27 for 0.7T, 20 and 8.7 for 1.1T and finally 7.2 and 2 for 1.5T. It means that the more anisotropic the sheets are, the higher the shifting effect is. The vibratory behaviour of the whole structure has also been investigated. An "Operating Deflection Shape" has been performed on one fourth of both shifted and non shifted CGO stacks for 1.1T and 1.5T. For 0.7T, the vibrations were too weak to be efficiently analyzed. The results are presented in Fig. 10(a) ($\beta = 0°$) and Fig. 10(b) ($\beta = 90°$) Fig. 11(a) and Fig. 11(b) show the 3D acceleration

of the whole structures for 1.5T respectively for $\beta = 0°$ and $90°$.

They put in evidence the reaction differences between the two configurations. The non-shifted stack presents counter-phased vibrations between the RD and TD. This is the usual vibration reaction of GO steels. On the other hand, the shifted stack presents in-phase vibrations between the RD and TD. Moreover, the vibrations for $\gamma = 45°$ are counter-phased.

The phase reference is set for $\gamma = 0°$ and the measured values corresponding to A_1, B_1, and $\gamma = 90°$, are presented in Fig.11. As previously mentioned, it can be noted that the axial and radial vibrations are in phase on both setups.

C. Radial Deformations

In the previous measurements, only the accelerations have been presented. In this part, the deformations of the CGO stacks are considered. In order to determine their nature, i.e. contraction or extension, the acceleration and the secondary voltage are used.

The waveforms of the flux density and deformations have been evaluated from formula 3 and 4 respectively.

$$B(t) = \frac{1}{n_2 S} \int v_2(t)dt \qquad (3)$$

$$\Delta l(t) = \int \int a(t)dt^2 \qquad (4)$$

For this evaluation, the integration constant is $\Delta l(t_0) = 0$ at $B(t_0) = 0$ T.
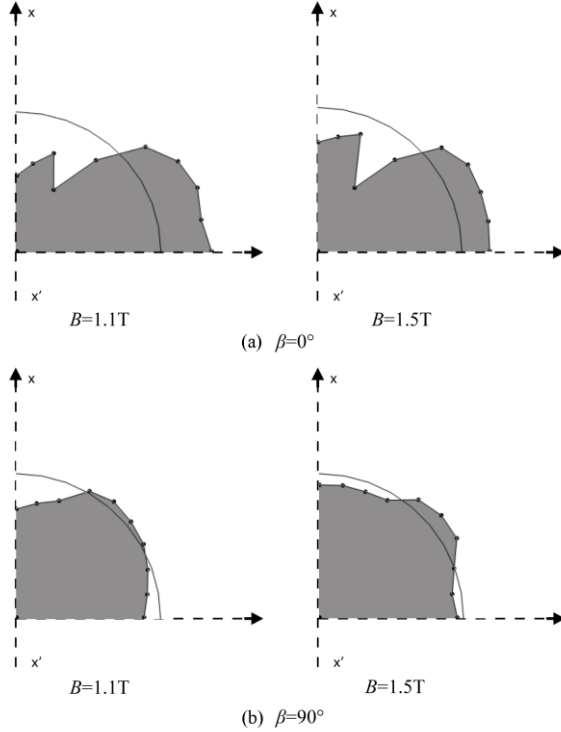

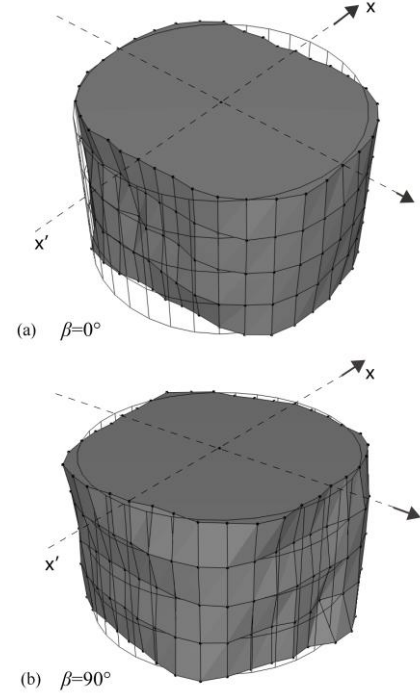Fig. 10.   Operating deflection shapes of radial vibrations (quarter of structure)

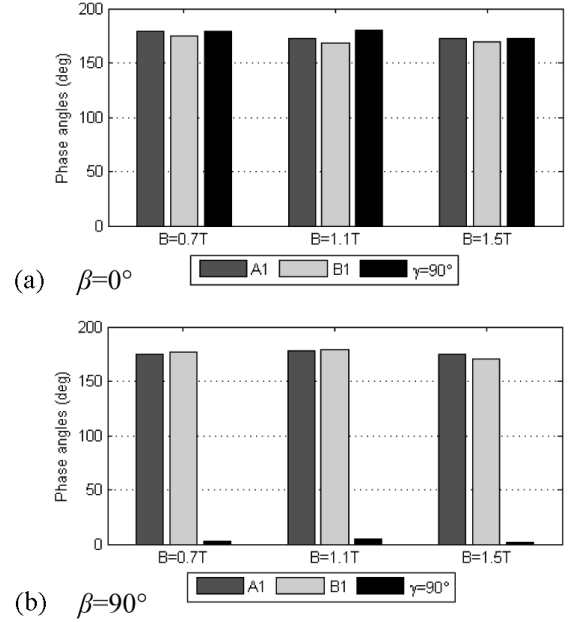Fig. 11.   Operating deflection shapes of radial vibrations for $B = 1.5T$

Fig. 12.   Phase angles between measurement points and γ=0°

The magnetostriction effect value with the magnetic flux density is presented in Fig. 13 for $\gamma = 0°$ and $90°$ and the CGO quality. The non-shifted setup presents a contraction along the RD and an elongation across the TD. This is the case for all the considered magnetic flux density values. For $\gamma = 0°$, the maximal displacement values of the shifted configuration are 26 (0.7T), 7 (1.1T), and 3 (1.5T) times lower than with the non shifted setup. As for $\gamma = 55°$, the magnetostriction effect

changes, it explains that, for $\gamma = 90°$, the nature of the displacement has changed: an elongation for the shifted setup and a contraction for the non-shifted device (Fig. 13). The amplitude of the displacements is lowered with the shifting. This is the case of the step lap transformer joint, where the GO laminations RD are crossed. The HGO stack presents the same phenomena but with a different level of vibration.

D. Local Analysis of the Flux Density

In previous measurements, the authors have presented the vibration variations of the 100 Hz component. However, the spectra in Fig. 14(a) for $\beta = 0°$ and in Fig. 14(b) for $\beta = 90°$ show that other components occur for the CGO non-shifted stack, although the supply is nearly sinusoidal. In order to understand the origin of these components, two experiments have been done to estimate the contribution of local saturations of the sheets and voltage harmonic components.

First, small coils, shown in Fig. 15, have been placed to analyse the flux density distribution in the sheets at $\beta=0°$, a zone where the magnetic flux is in the TD giving the higher magnetostrictive vibrations. The displacements are measured at $\gamma = 0°$.
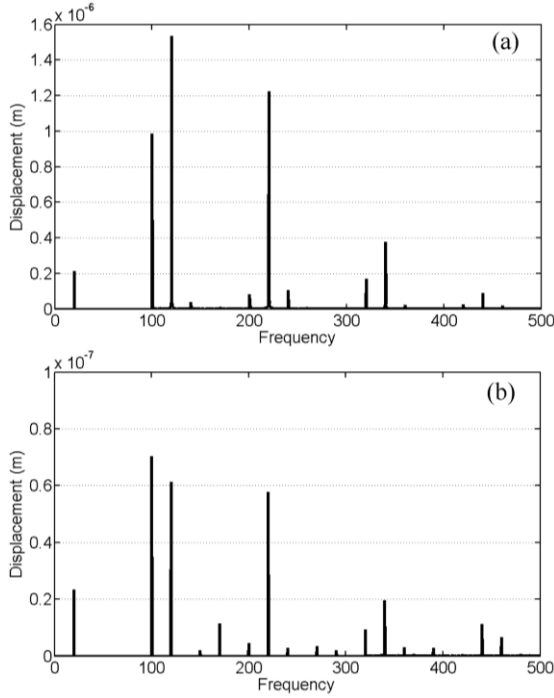
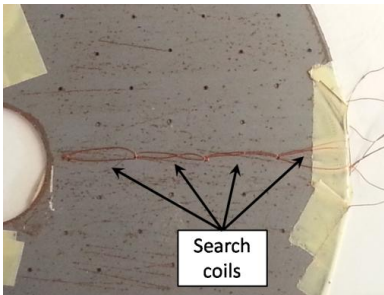Fig. 14. Displacements of the CGO non-shifted stack for $\beta = 0°$ (a) and $\beta = 90°$ (b)

Fig. 15. Search coils

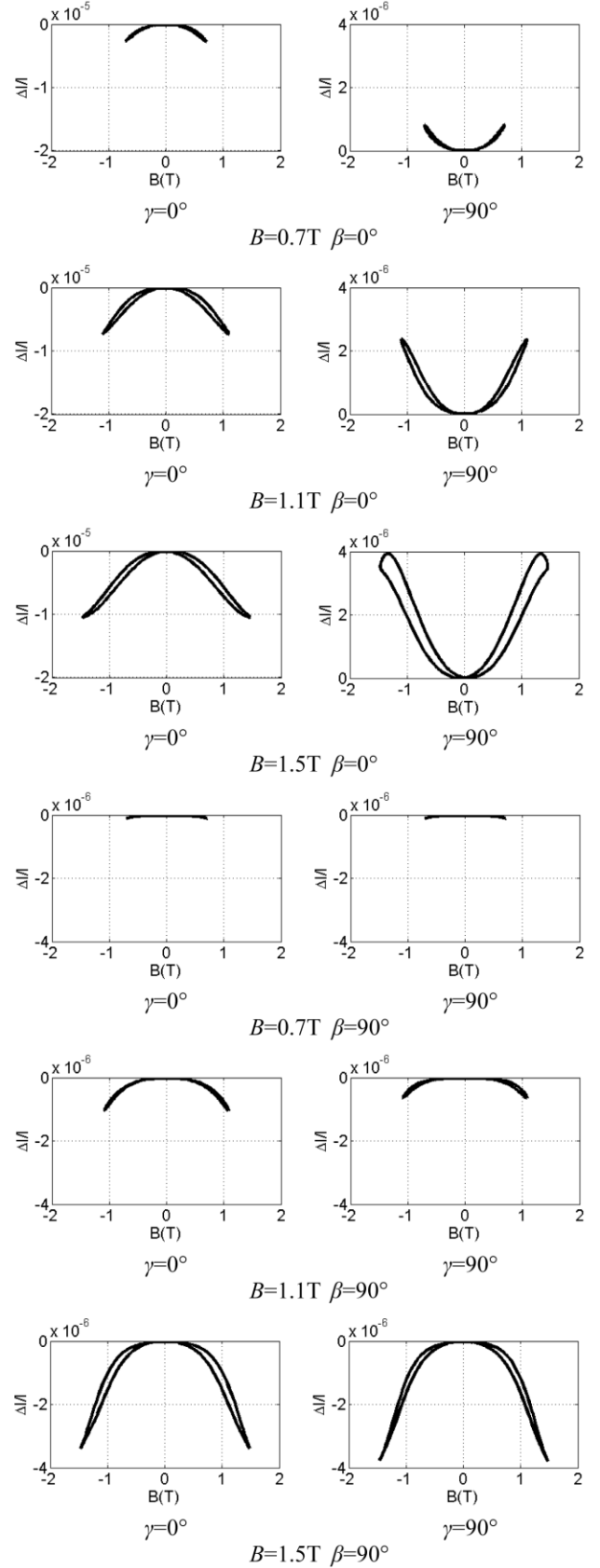Fig. 13. Radial displacements along $\gamma = 0°$ and $\gamma = 90°$

Second, to evaluate the supply influence, a voltage component has been superimposed to the 50Hz fundamental. The chosen frequency of this harmonic is 170Hz in order to distinguish clearly the impact of the additional voltage from eventual magnetic saturations components of frequency multiple of 50Hz [26]. This frequency, close to the third excitation harmonic, can come from the grid or the power electronic [27]. The amplitudes of the sinusoidal 50Hz and 170Hz lead to average magnetic flux densities of 0.4T and 0.2T respectively, as shown in Fig. 16.
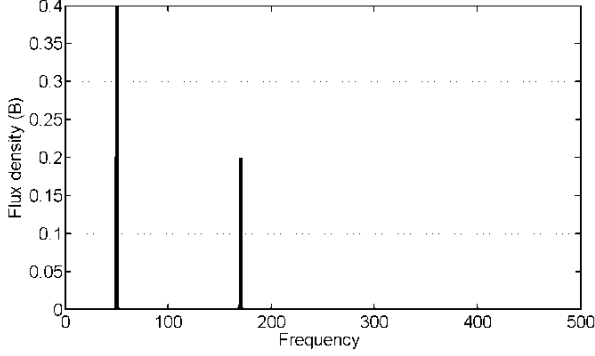

Fig. 16. Flux density for $\beta=0°$ and $\beta=90°$

The local measurement of the flux density show, for $\beta= 0°$ in Fig. 17(a) and for $\beta=90°$ in Fig. 18(a), a higher spectral content: components of major amplitude appear at 150Hz (due to the saturation) and also the frequency created with the intermodulation products (IM3) of the excitation caused by the non-linearity of the material: 70Hz (170-2x50), 270Hz (2x50+170), 290Hz (2x170-50) and 390Hz (2x170+50). As the displacements due to the magnetostriction are proportional to the square of the flux density, the square of magnetic flux density spectrum has been determined, as shown in Fig. 17(b) and in Fig. 18(b).

There are great similarities between the acceleration (Fig. 14) and the square of magnetic flux density calculated from the local flux density (Fig. 17(b)). The frequencies of the displacement components can be clearly explained by considering two flux density harmonic components of frequency f_1 and f_2. When multiplied, two components of frequency $f_1 - f_2$ and $f_1 + f_2$ appear. That explains that:

- The components visible in the average flux density spectrum generate vibrations at 100Hz (2x50Hz), 120Hz (170Hz-50Hz), 220Hz (170Hz+50Hz) and 340Hz (2x170Hz).
- The local saturation introduces additional components at the origin of two kinds of vibrations. The first leads to components already in the spectrum at frequencies:
  - 100Hz (150Hz - 50Hz; 170Hz - 70Hz; 270Hz - 170Hz and 390Hz - 290Hz).
  - 120Hz (170Hz - 50Hz; 270Hz - 150Hz and 290Hz - 170Hz), 220Hz (170Hz + 50 Hz; 270Hz - 50Hz; 290Hz - 70Hz and 390Hz - 270Hz).
  - 340Hz (2x170Hz and 70Hz + 270Hz).

The second concerns components of different frequencies: 20Hz (70Hz - 50Hz), 200Hz (50Hz + 150Hz), 240Hz (170Hz + 70Hz) and 320Hz (170Hz + 150Hz).

As a consequence, the local sensors allow measuring local saturations responsible of vibrations components as well as those due to the voltage harmonics.
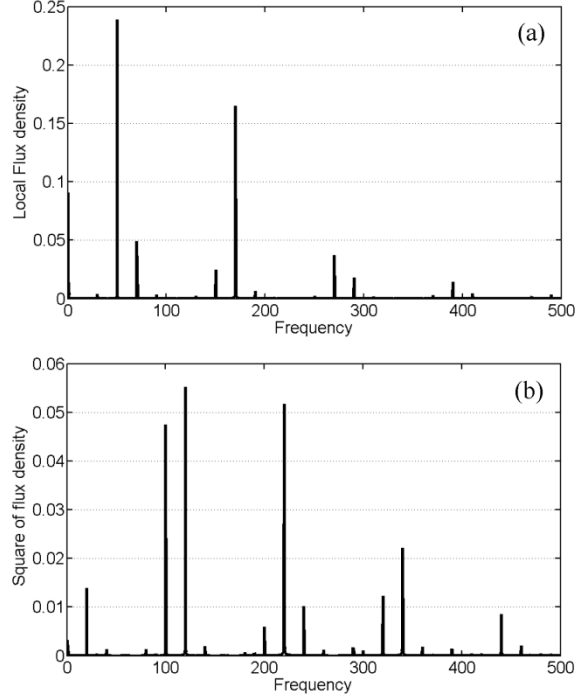

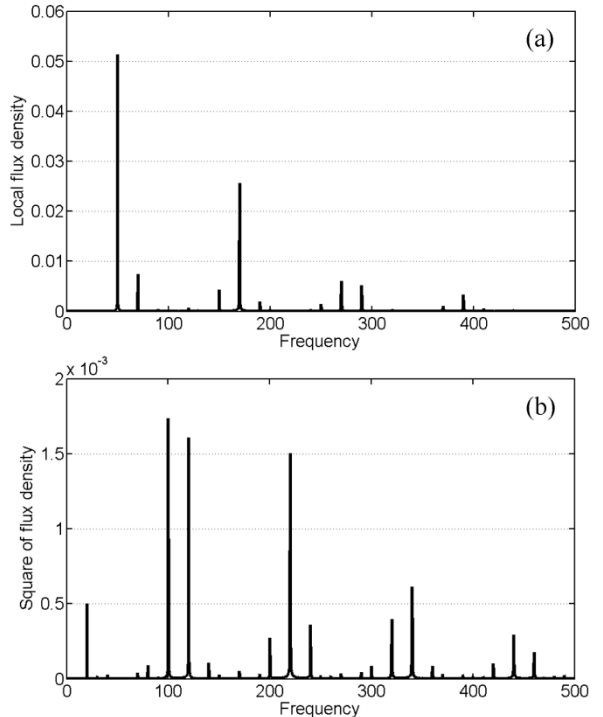Fig. 17. Spectrum of the local flux density (a) and its square (b) for $\beta=0°$

Fig. 18. Spectrum of the local flux density (a) and its square (b) for $\beta=90°$

It can be noted in Fig. 17(a) and 18(b) that all the vibrations measured in the TD are, as for the 100Hz component, greatly reduced compared to the RD.

V. Conclusion

The measurement results presented in this paper provide interesting information about magnetostriction and Maxwell's forces effects. Although, in this study, the in plane Maxwell's forces at the corner joints of the step lap have not been modelled, it seems to give some hints towards explanation for vibration mechanisms inside transformer core, particularly at the joints. The important result, which can be extracted from this analysis, is that both Maxwell's force and magnetostriction effects are, concerning the vibrations, of same order of magnitude. That leads to questions about the contribution of noise generated by the transformers. The legs generate magnetostrictive noise whereas the Maxwell's forces and the magnetostriction which occur in the corners may be partially compensated. Then, small coils allow measuring local saturations. It has been shown that they lead to vibrations of non negligible amplitude. Moreover, the vibration spectral may be greatly enhanced if the supply is not sinusoidal.

References

[1] C. Bengtsson, "Industrial significance of losses and noise", in Proc. *1&2DM*, Vienna, Austria, 2012, pp.13-14.

[2] K. Majer, "The analysis of the vibrations of the cores of model transformers," in *Proc. ISEF,* Arras, France, 2009, pp. 587-588.

[3] B. Weiser, A. Hasenzagl, T. Booth, and H.Pfutzner, "Mechanisms of noise generation of model transformer cores," *J. Magn. Magn. Mater*., vol. 160, pp. 207-209, 1996.

[4] A.J. Moses, "Measurement of magnetostriction and vibration with regard to transformer noise," *IEEE Trans. Magn.,* vol. 10, no. 2, pp. 154- 156, Jun. 1974.

[5] W. Kubiak, P Witczak, "Vibration analysis of small power transformer," in Proc. *ISEF*, Arras, France, 2009, pp. 581-582.

[6] G. Loizos, A.G Kladas. "Core Vibration Analysis in Si-Fe Distributed Gap Wound Cores," *IEEE Trans. Magn.,* vol. 48, no. 4, pp. 1617-1620, Apr. 2012.

[7] L. Vandevelde, J.A.A. Melkebeek, "Magnetic forces and magnetostriction in electrical machines and transformer cores," *IEEE Trans. Magn.,* vol. 39, no. 3, pp. 1618- 1621, May 2003.

[8] R. Penin, J.-P. Lecointe, G. Parent, J.-F. Brudny, T. Belgrand, "Estimation of relative magnetostriction and Maxwell's forces in stacked Grain Oriented steel structures," in Proc. *ICEM*, 2012, pp. 1971-1976.

[9] Magnetic core and use of magnetic core for electrical machines, by J.F. Brudny, B. Cassoret, R. Lemaître, and J.-N. Vincent. (2009, Mars 12). *Patent WO 2009/030 779 A1*.

[10] X. She, A. Huang, F. Wang, R. Burgos, "Wind Energy System with Integrated Functions of Active Power Transfer, Reactive Power compensation, and Voltage conversion," *IEEE Trans. Ind. Electron*., vol.60, no.10, pp.4512-4524, Oct. 2013.

[11] S. Iida, Y. Okuma, "S. Masukawa, ; S. Miyairi, B.K. Bose, "Study on magnetic noise caused by harmonics in output voltages of PWM inverter*," IEEE Trans. Ind. Electron.*, vol. 38, no. 3, pp. 180-186, Jun 1991.

[12] T.D. Kefalas, A.G. Kladas, "Harmonic Impact on Distribution Transformer No-Load Loss," *IEEE Trans. Ind. Electron*., vol. 57, no. 1, pp. 193-200, Jan. 2010.

[13] B. Weiser, H. Pfutzner, and J. Anger, "Relevance of magnetostriction and forces for the generation of audible noise of transformer cores," *IEEE Trans. Magn*., vol. 36, no. 5, pp. 3759-3777, Sept 2000.

[14] G.E. Mechler, R.S. Girgis, "Magnetic flux distributions in transformer core joints," *IEEE Trans. Power Del.*, vol. 15, no. 1, pp.198-203, Jan 2000.

[15] T. Nakata, N. Takahashi, Y. Kawase, "Magnetic performance of step-lap joints in distribution transformer cores," *IEEE Trans. Magn.*, vol. 18, no. 6, pp. 1055- 1057, Nov. 1982.

[16] S. Arai, M. Mizokami, and M. Yabumoto, "Magnetostriction of grain oriented Si-Fe and its domain model," *Przeglad Elektrotechniczny*, vol. 87, no. 9b, pp. 20-23, 2011.

[17] J. Shilling, G. Houze, "Magnetic properties and domain structure in grain-oriented 3% Si-Fe," *IEEE Trans. Magn.*, vol. 10, no. 2, pp. 195-223, Jun. 1974.

[18] A. Hasenzagl, B. Weiser, H. Pfützner, "Magnetostriction of 3% SiFe for 2-D magnetization patterns," *J. Magn. Magn. Mater.* vol. 160, pp. 55-56, July 1996.

[19] H. Yamaguchi, H. Pfützner, and A. Hasenzagl. "Magnetostriction measurement on the multidimensional magnetization performance of SiFe steel", *J. Magn. Magn. Mater.*, vol. 320, pp.618-622, 2008.

[20] D. Wakabayashi, T. Todaka, Takashi, and M. Enokizono, "Measurement of Three-Dimensional Magnetostriction on Grain-Oriented Electrical Steel Sheet," *Journal of Electrical Engineering*, vol. 62, no. 3, pp.153, 2011.

[21] W. Kitagawa, K. Fujiwara, Y. Ishihara, "Structure deformation analysis caused by magnetostriction of magnetic steel sheet using combination of Electromagnetic and Structure analysis," in Proc. *ICEM*, Rome, Italy, 2010, pp.1-6.

[22] G. Parent, R Penin, J.P. Lecointe, J.F. Brudny, and T. Belgrand, "Analysis of the Magnetic Flux Distribution in a New Shifted Non Segmented Grain Oriented AC Motor Magnetic Circuit," *IEEE Trans. Magn.*, vol. 49, no. 5, pp. 1977-1980, May 2013.

[23] ThyssenKrupp Electrical Steel: Our products-grain oriented steel PowerCore. 2010.

[24] S. Taguchi, T. Yamamoto, A. Sakakura,"New grain-oriented silicon steel with high permeability "ORIENTCORE HI-B"," *IEEE Trans. Magn.,* vol. 10, no 2, pp. 123-127, Jun 1974.

[25] C. Demian, B. Cassoret, J.F. Brudny, T. Belgrand, "AC magnetic circuits using non segmented shifted grain oriented electrical steel sheets: impact on induction machine magnetic noise," *IEEE Trans. Magn.*, vol. 48, no. 4, pp. 1409-1412, Apr 2012.

[26] J.P. Lecointe, B. Cassoret, and J.F. Brudny, "Distinction of toothing and saturation effects on magnetic noise of induction motors," *Progress In Electromagnetics Research,* vol. 112, pp. 125-137, 2011.

[27] P. Chaturvedi, S.Jain, P. Agarwal, "Carrier Based Neutral Point Potential Regulator with Reduced Switching Losses for Three-Level Diode Clamped Inverter," *IEEE Trans. Ind. Electron*., in press.
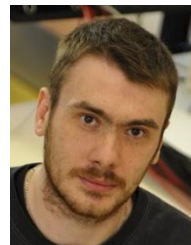
Rémi Penin was born in Armentières (France), in 1986. He received master degree in 2009 from University of Artois (France). He is now Ph.D. student at the University of Artois (LSEE). His research interest is the core losses and the vibrations in transformers.

Jean-Philippe Lecointe, DSc, received the MSc degree in Electrical Engineering from the Université des Sciences et Technologies de Lille, France, in 2000. He received the PhD degree from the Université d'Artois, France, in 2003. He is currently Associate Professor at the Artois University and he joined the institute LSEE (Electrical Systems and Environment Research Laboratory), France. His research interests focus on electromagnetic design, efficiency, noise and vibrations of electrical machines

Guillaume Parent was born in Strasbourg, France. He received the Ph.D. degree in electrical engineering jointly from the University of Lille, Lille, France, and the University of Liège, Liège, Belgium, in 2008. He is currently an Associate Professor of electrical engineering at the Artois University, Béthune. His main research interests include electromagnetic analysis with the Finite-element method and noise analysis in electromagnetic systems and vibrations.

Jean-François Brudny (M'92–SM'04) received the Ph.D. and the D.Sc. degrees from Lille University, Lille, France, in 1984 and 1991, respectively. Since 1992, he has been with the Universite d'Artois, Béthune, France, where he was a Full Professor and is currently the Head of the Laboratoire Systèmes Electrotechniques et Environnement (EA 4025). His research interests include noise and vibrations of electromechanical systems and new designs for efficiency increase of ac rotating electrical machines.

Thierry Belgrand received the Ph.D. degree in materials science from the University of Lille in 1987. He is currently Head of R & D - TKES UGO.